JOURNAL OF Applied Polymer SCIENCE

Fabrication of bimodal porous PLGA scaffolds by supercritical CO_2 foaming/particle leaching technique

Xin Xin, Qian-Qian Liu, Chuan-Xin Chen, Yi-Xin Guan, Shan-Jing Yao
College of Chemical and Biological Engineering, Zhejiang University, Hangzhou 310027, China
Correspondence to: Y.-X. Guan (E-mail: guanyx@zju.edu.cn)

ABSTRACT: Specific pore structure is a vital essential for scaffolds applied in tissue engineering. In this article, poly(lactide-*co*-glycolide) (PLGA) scaffolds with a bimodal pore structure including macropores and micropores to facilitate nutrient transfer and cell adhesion were fabricated by combining supercritical CO_2 ($scCO_2$) foaming with particle leaching technique. Three kinds of NaCl particles with different scales (i.e., 100–250, <75, <10 μm) were used as porogens, respectively. In particular, heterogeneous nucleation occurred to modify $scCO_2$ foaming/particle leaching process when NaCl submicron particles (<10 μm) were used as porogens. The observation of PLGA scaffolds gave a formation of micropores (pore size <10 μm) in the cellular walls of macropores (pore size around 100–300 μm) to present a bimodal pore structure. With different mass fractions of NaCl introduced, the porosity of PLGA scaffolds ranged from 68.4 ± 1.4 to 88.7 ± 0.4% for three NaCl porogens. The results of SEM, EDS, and *in vitro* cytotoxicity test of PLGA scaffolds showed that they had uniform structures and were compatible for cell proliferation with no toxicity. This novel $scCO_2$ foaming/particle leaching method was promising in tissue engineering due to its ability to fabricate scaffolds with precise pore structure and high porosity. © 2016 Wiley Periodicals, Inc. J. Appl. Polym. Sci. **2016**, *133*, 43644.

KEYWORDS: biomedical applications; foams; synthesis and processing

Received 24 November 2015; accepted 11 March 2016
DOI: 10.1002/app.43644

INTRODUCTION

Tissue engineering is a technical hotspot that aims to repair diseased or damaged tissues via a combination of cell/molecular biology and materials chemistry/engineering. In the development of tissue engineering, scaffold is considered to be a vital essential as a three-dimensional template for cells adhesion, proliferation, and differentiation.[1–4] Materials used to prepare scaffolds matrix range from stiff inorganic materials to synthetic polymeric materials. Aliphatic polyesters, such as polylactide and poly(lactide-*co*-glycolide) (PLGA), produced with predictable and reproducible features, have gained much attention and the approval of FDA.[5] In general, high porosity, specific pore structure and suitable mechanical properties are required for tissue engineering scaffolds.[6–9] As a fine implant for therapy, scaffolds should also provide appropriate microenvironment and good biocompatibility.

In recent years, there have been intense efforts to fabricate ideal scaffolds with specific surface area, high porosity, and favorable mechanical properties for different applications.[10–13] Hollister[4] and Mou *et al.*[10] reported pores with the size of 10 to 1,000 μm played a significant role in tissue regeneration by preserving tissue volume, providing temporary mechanical function and delivering biofactors. Furthermore, the combination of macro- and micropores renders scaffolds suitable for cell proliferation and migration, as well as for protein and nutrient uptake in new tissue vascularization.[1] The scaffolds not only have to provide a pore size range and suitable porosity for cell adhesion and mass transport, but also to meet the mechanical strength of a modulus of 10–1,500 MPa for hard tissues or 0.4–350 MPa for soft tissues.[4]

Scaffolds with diverse morphological characteristics can be fabricated by different methods such as phase separation,[5] injection molding,[14] compression molding,[15,16] solvent casting/particle leaching,[8] gas foaming,[9] and so forth. Among all of these methods, supercritical CO_2 ($scCO_2$) foaming has recently achieved great emphasis for avoiding the use of organic solvents. Furthermore, the rather low critical temperature (31.1 °C) and pressure (7.4 MPa) of CO_2 may also offer a new way to load growth factors onto polymer matrix in a single step.[17,18] At the same time, $scCO_2$ foaming technique tends to obtain coherent macro- or microstructural scaffolds compared with conventional scaffold fabrication techniques. Ozdemir *et al.*[19] reported that scaffolds fabricated by $scCO_2$ foaming proved to be an ideal support for cell attachment owing to the presence of both nano- and micropores, and many available scaffolds were fabricated via $scCO_2$ foaming.[20,21]

The potential drawback of $scCO_2$ foaming method, however, has been noted because of a lack of interconnectivity between pores (open pore number limited to between 10 and 30% of the total pore number). Therefore one supplement with other pore-forming strategy may be necessary, and Quirk *et al.*[17] believed that $scCO_2$ would result in an innovative approach with the combinations of other methods. For instance, particle leaching technique has been previously used to fabricate scaffolds with high interconnectivity.[22–24] Using thermoplastic zein as a porogen, Salerno *et al.*[1] successfully made porous scaffolds for bone regeneration via $scCO_2$ foaming and particle leaching techniques. In addition to thermoplastic zein chosen as the porogen, paraffin spheres,[24] sugar particles,[25] and inorganic salt particles, especially sodium chloride (NaCl), are commonly used by researchers due to their facile sourcing and easy leaching.[26–29] As for NaCl porogen, NaCl particles with the size of several hundred micrometer or about 5 μm were used to prepare scaffolds individually. But the nucleation mechanism was rarely involved considering different sizes of NaCl particles. Meanwhile the effect of different NaCl particles size on the structure of scaffolds needed to be thoroughly studied.

In this study, PLGA scaffolds with bimodal pore structure are fabricated by $scCO_2$ foaming/particle leaching technique, in which NaCl particles with three different dimensions are chosen as the porogen since the size and mass fraction of NaCl particles would greatly influence the structure of scaffolds. The effect of operation parameters and porogen on scaffolds is investigated in detail, and porosity, mechanical property and *in vitro* cytotoxicity of scaffolds are characterized. Specifically, the nucleation behavior is taken into account for submicron NaCl particles as the porogen.

EXPERIMENTAL

Materials

PLGA (lactide:glycolide = 85:15, M_w = 140K, PDI = 1.73) in a granular form was purchased from Shenzhen Bright China Industrial (Shenzhen, China). Cell line of MC3T3-E1 Subclone 14 was supplied from Cell Bank of Chinese Academy of Sciences (Shanghai, China). MTT test kit, fetal bovine serum, penicillin, and streptomycin solution were obtained from Sangon Biotech (Shanghai, China). MEMα medium (GIBCO 12571-063) was from GIBCO (California). All other chemicals were of reagent grade and utilized without further purification.

Preparation of PLGA Samples

First, 1.0 g of PLGA granule was dissolved in 10 mL dichloromethane to obtain PLGA solution. Then the polymer solution was added to 1% polyvinyl alcohol aqueous solution, and the mixed solution was processed by a high-speed shearing machine and heated in a thermostatic water bath at 30 °C to evaporate dichloromethane. The PLGA microspheres could be obtained after centrifugation and freeze-drying. In this work, three sizes of NaCl particles were used as porogens, which were obtained through different methods, that is, sieving, grinding/sieving, and spray-drying. Finally, the mixtures of PLGA microspheres and NaCl particles in a certain proportion were mold-pressed at 20 MPa in a die for 2 min to get cylindrical flakes. The thickness of the flakes was limited to 0.6 mm with a diameter of 13 mm by 0.05 g.

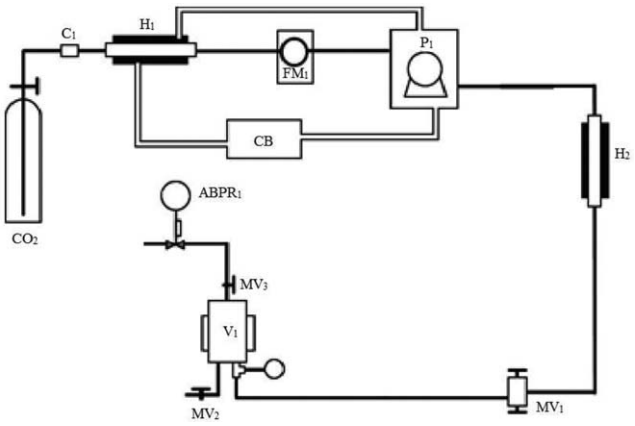

Figure 1. Schematic diagram of the supercritical carbon dioxide foaming process. ABPR1, automated back pressure regulator; C1, check valve; CB, cooling bath; FM1, flow meter; H1, H2, heat exchanger; MV1-MV3, manual valve; P1, pump; V1, autoclave).

The $scCO_2$ Foaming Process

Supercritical system (SFE-500MR-2-FMC 10) was used in the foaming process. The technological flow sheet was shown in Figure 1, and it was mainly consisted of an autoclave of 50 mL. In this experiment, specified weight of PLGA flakes with different NaCl fractions were put into the autoclave, where CO_2 pressure and temperature were maintained at constant values. Temperature fluctuation was controlled to be ± 1 °C and pressure fluctuation ± 1 MPa. After equilibrating for 2 h, the CO_2 pressure was reduced to ambient pressure at a rate of approximately 0.2 MPa/s, and the foams could be removed from the autoclave. Then the samples were transferred into distilled water for 72 h to leach out NaCl particles in a vibrator. After dialyzed and freeze-dried at -50 °C overnight, the prepared scaffolds were stored in a desiccator for further analysis.

Characterization

The morphologies of porous scaffolds and NaCl particles were obtained by scanning electron microscopy (SEM) (JSM-6390A, JEOL, Japan). The scaffolds were freeze-fractured in liquid nitrogen, sputter-coated with gold and operated at an accelerating voltage of 25 or 30 kV. The pore sizes of PLGA scaffolds and the sizes of NaCl particles were analyzed by image processing analysis software (Image Pro Plus 6.0, Media Cybernetics, America). The porosities of scaffolds were obtained using mercury intrusion porosimetry (AutoPore IV 9500 V1.07, Micromeritics). The size of minimum pore, which mercury could permeate into, reduced with the increase of intrusion pressure. The static compression properties of scaffolds were measured using a material testing machine (Zwick/Roell Z2.5, Zwick/Roell, Germany) working at a compression rate of 0.5 mm/min, and equipped with a 2-kN loading cell. The compression modulus (E) was the slope of the initial linear part by depicting the curve of stress versus strain relationship. Energy dispersive X-ray spectroscopy (EDS) was used to detect the residual of NaCl.

In Vitro Cytotoxicity Test of PLGA Scaffolds

A sample of 0.1 g PLGA scaffold was soaked in 2 mL of MC3T3-E1 Subclone 14 cell culture solution and shaken at 37 °C for 24 h in an isothermal vibrator after sterilization. Then, the liquid extract could be obtained by filtering out the PLGA samples and

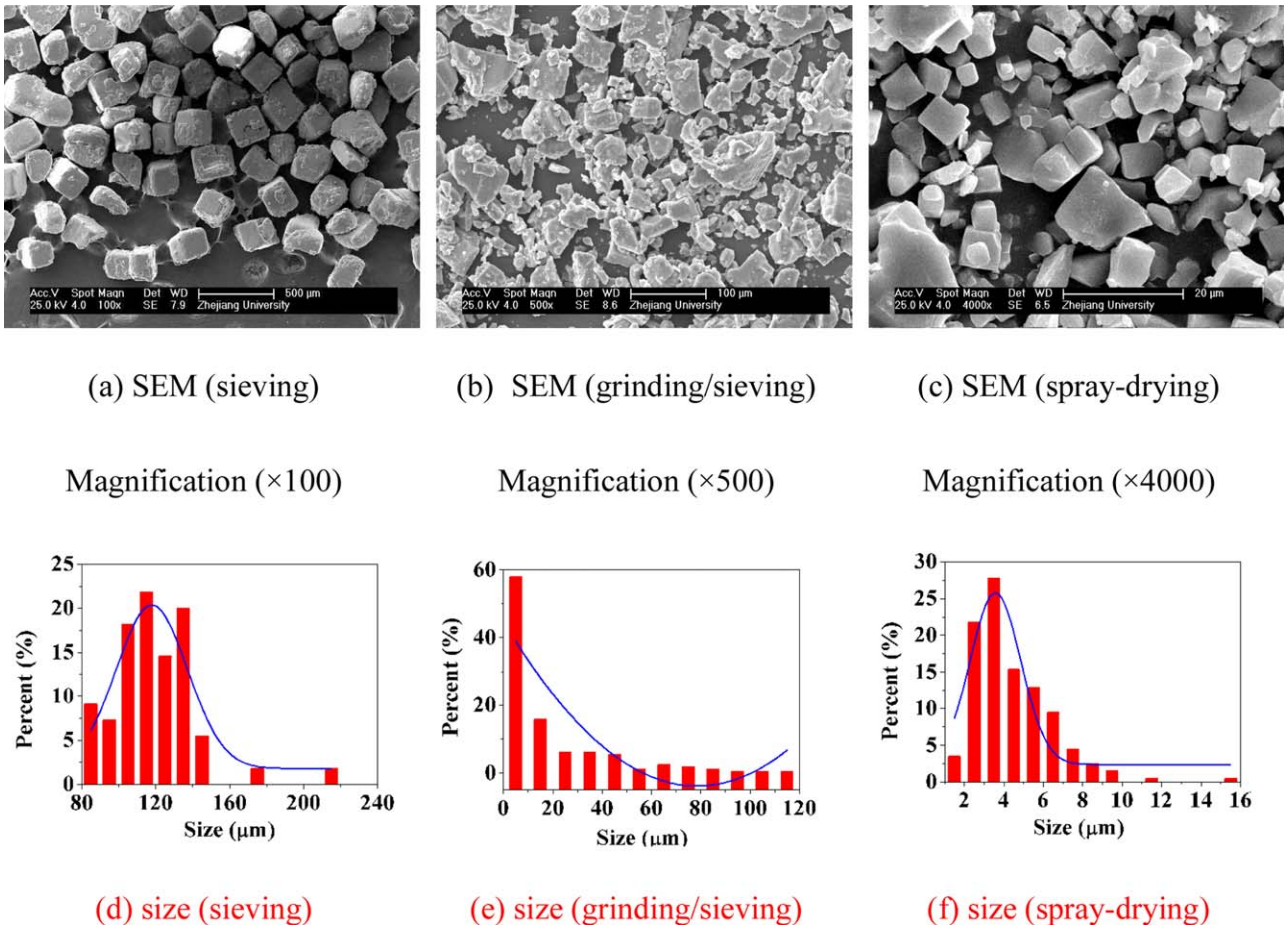

Figure 2. Morphologies and size distributions of NaCl particles as porogen prepared by sieving in (a,d), grinding/sieving in (b,e), and spray-drying in (c,f), respectively. [Color figure can be viewed in the online issue, which is available at wileyonlinelibrary.com.]

ready for later assay. For the cytotoxicity test, a cell density of 1 $\times$ 10^4 cells/mL culture medium was used and inoculated to 24-well cell culture plates with each well containing 400 μL cell suspension. After 48 h culture at 37 °C under 5% CO_2 atmosphere, the cell culture solution was removed and each well was rinsed two to three times with PBS solution. Then 400 μL liquid extract per well were added as experimental groups; in a parallel, 400 μL cell culture solution as negative control, and 400 μL cell culture solution containing 6% phenol as positive control. Cells were cultured at 37 °C under 5% CO_2 atmosphere again. After 24 h incubation, 40 μL MTT (5 mg/mL) was added to each well for a further culture of 4 h, and then 40 μL DMSO was added to each well in replacement of the medium. Finally, assessment of cytotoxicity was done by photocolorimetric method at 570 nm and the cell relative growth rate (RGR) of each group was compared. The RGR could be calculated as follows:

$$\mathrm{RGR}\,(\%) = \frac{\text{average absorbancy of experimental groups}}{\text{average absorbancy of negative groups}} \quad (1)$$

RESULTS AND DISCUSSION

Fabrication of PLGA Scaffolds Using scCO$_2$ Foaming/Particle Leaching Process

Generally, operation parameters of scCO$_2$ foaming process include foaming temperature (T), pressure (P), saturation time and depressurization rate, and so forth. Based on our previous study,[21] a saturation time of 2 h was verified to be adequate to allow complete saturation of CO_2 in PLGA before quenching with a depressurization rate of 0.2 MPa/s. For the particle leaching process, NaCl particles with different sizes were used as the porogen in this experiment. The morphologies and size distributions of NaCl particles with different pretreatment methods were shown in Figure 2, respectively. We can see that sieved NaCl particles had a structure of regular cuboid, while NaCl particles (ground/sieved, spray-dried) had a structure of irregular polygon. As for particles distribution, 83.64% of sieved NaCl particles had a size of 100–250 μm, and 99.01% of spray-dried particles smaller than 10 μm. However, the ground/sieved NaCl particles had a wide distribution, of which 96.95% were $<$75 μm. In this work, the effects of process parameters including foaming temperature and pressure, the sizes and mass fractions of NaCl particles on pore structures of PLGA scaffolds were studied in detail, which were summarized in Table I.

Effect of Foaming Temperature on Scaffolds. According to our previous work,[21] PLGA scaffolds with large polygonal cells or a high density of pore could be fabricated when the foaming temperature was below 45 °C or above 65 °C. Therefore, 45 and 65 °C were typically chosen as foaming temperature in this experiment when 60% NaCl was added as the porogen with the particles sizes of 100–250 μm. The SEM micrographs of PLGA

Table I. Summary of Operating Parameters of $scCO_2$ Foaming/Particle Leaching

No.	Sizes of NaCl particles (μm)	Mass fractions of NaCl % (w/w)	Temperature (°C)	Pressure (MPa)
Influence of foaming temperature (*T*)				
1	100–250	60	45	15
2	100–250	60	65	15
Influence of foaming pressure (*P*)				
3	100–250	60	45	15
4	100–250	60	45	20
Influence of sizes of NaCl particles				
5	100–250	60	45	15
6	<75	60	45	15
7	<10	60	45	15
Influence of mass fractions of NaCl				
8	100–250	60	45	15
9	100–250	80	45	15
10	100–250	90	45	15
11	<75	60	45	15
12	<75	80	45	15
13	<75	90	45	15
14	<10	5	35	15
15	<10	10	35	15
16	<10	20	35	15

scaffolds with the porogen at different foaming temperatures were shown in Figure 3. From Figure 3(a) at temperature of 45 °C, PLGA scaffolds were consisted of two kind of pores, namely large pores by leaching out of NaCl particles or small pores by $scCO_2$ foaming, which was clearly shown in Figure 3(b) for the magnification of PLGA matrix. Furthermore, the scaffolds morphologies did not show significant difference when the temperature was elevated to 65 °C in Figure 3(c).

In the foaming process, the increase of temperature would lead to the increase of the CO_2 diffusivity in PLGA matrix but the decrease of CO_2 solubility. In other words, at a higher temperature the growth of pores was faster, while fewer nuclei were formed. The net effect of these two contrary factors was an increase in the pore diameter with the increase of temperature.[30] Nevertheless, the experimental results indicated that these effects were likely negligible with the presence of porogen. The addition of NaCl particles enhanced the rigidity of the substrate, namely, making PLGA less sensitive to a temperature shift. Hence, the dependence of pore diameters of scaffolds on the temperature was not notable while the porogen of NaCl was added.

Effect of Foaming Pressure on Scaffolds. With the addition of NaCl particles, the SEM micrographs of scaffolds at different foaming pressures were also shown in Figure 3. We can see that the diameters of PLGA pores produced by $scCO_2$ foaming decreased slightly when the pressure was increased from 15 to 20 MPa [Figure 3(d)].

When CO_2 solubility in PLGA increased at higher pressure, there was more CO_2 available for the nucleation and growth of pores.[31] Thus, the key factor that controlled the pores diameter was the generation of more nuclei as pressure increased. As a result, a large number of smaller pores were obtained. That is to say, even though NaCl particles were used as the porogen, the change of CO_2 solubility with the increase of pressure still had certain effect on the pore diameter.

Effect of Diameters and Mass Fractions of NaCl Particles on Scaffolds. In the foaming process, the sizes of NaCl particles had a great impact on the sizes and structures of pores. At the addition of NaCl particles of 60% (w/w), the SEM micrographs of scaffolds foamed at 45 °C and 15 MP using different sizes of NaCl porogen (<75 and <10 μm) were shown in Figure 4. As shown in Figure 4(a), the pore size of scaffolds presented a bimodal distribution when the size of NaCl particles was below 75 μm, which is quite similar with Figure 3(a) with NaCl particles of 100–250 μm. The square macropores well replicated the shape and size of the raw NaCl particles and the micropores of around 20 μm were produced by $scCO_2$ foaming. However, when the sizes of NaCl particles reached below 10 μm, more small pores were formed by leaching out of submicron NaCl particles, as shown in Figure 4(b).

This phenomenon was most likely due to the influence of the addition of different sizes of NaCl particles in the foaming process. The presence of stiff NaCl particles (especially large ones) prevented the growth of gas nuclei in PLGA matrix, which resulted in the formation of small pores around NaCl particles. After the leaching approach, the volume occupied by the NaCl particles remained and the square

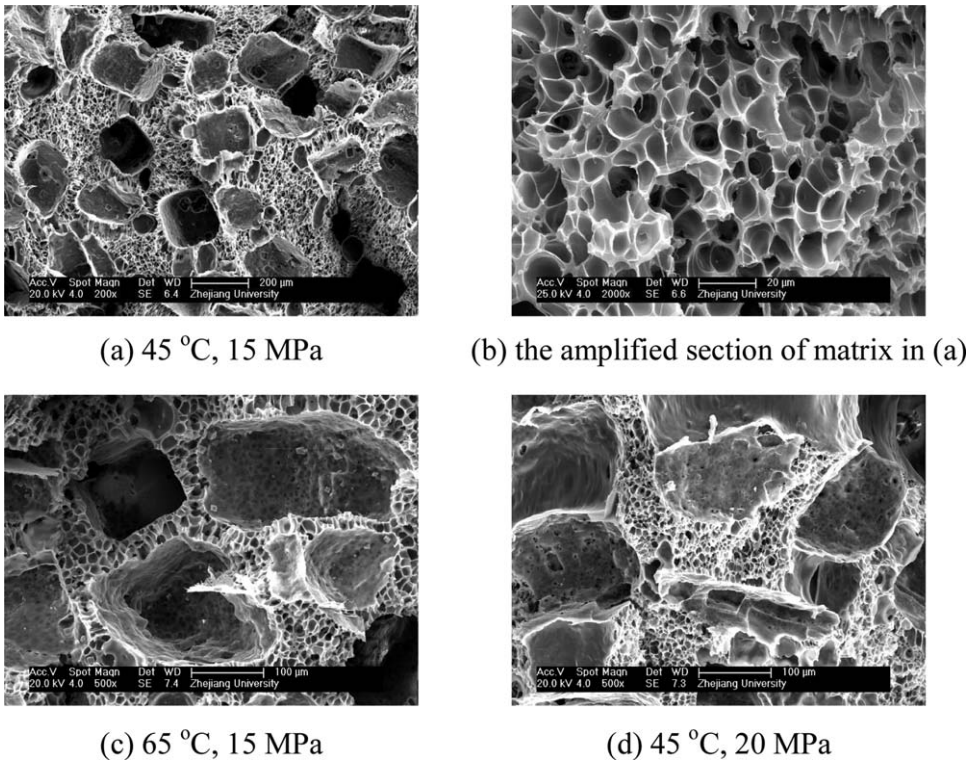

Figure 3. Effects of foaming temperature and pressure on the formation of pores of PLGA scaffolds with the addition of NaCl porogen (NaCl particles sizes of 100–250 μm, NaCl mass fraction of 60%).

macropores were formed. With the decrease of size of NaCl particles, the specific surface area of these NaCl particles increased to further weaken the interactions between PLGA and $scCO_2$. Under this situation, pores produced by $scCO_2$ foaming tended to be even smaller. Hence, when the size of NaCl particles was below 10 μm, both of small pores produced by leaching out of NaCl particles and by $scCO_2$ foaming were formed.

The influence of NaCl mass fractions on scaffolds using different sizes of NaCl particles was conducted in this experiment, and the results were also shown in Figure 4. The ratio of PLGA micropores obviously decreased and more irregular macropores were formed when the mass addition of NaCl was increased from 60 to 90%. With the rise of NaCl fractions, the mass of foaming material PLGA decreased accordingly, and the interactions between PLGA and $scCO_2$ weakened due to the presence of stiff NaCl particles, thus less micropores resulted from $scCO_2$ foaming were observed. At NaCl mass fraction of as high as 90%, PLGA was only considered to sustain the integrity of scaffolds [Figure 4(d,f)].

As shown above, bimodal porous PLGA scaffolds were successfully prepared using NaCl as porogen, in which macropores obtained during the leaching step were uniformly distributed within micropores of PLGA network. Specifically, when the size of NaCl particles was 100–250 μm, macropores were surrounded by micropores with diameter less than 20 μm. This kind of bimodal structure was essential to permit cell and tissue ingrowths and delivery of nutrient substance.[1]

Nucleation Mechanism using Submicron NaCl Particles

From Figure 4(b), more small pores were observed when submicron NaCl particles (<10 μm) were used as the porogen. Furthermore, scaffolds were fabricated by adding different amounts of submicron NaCl particles and the results were shown in Fig 5. When the amount of NaCl was 5 or 20%, scaffolds with micropores (pore diameter < 10 μm) in the cellular walls of macropores (pore size around 100–300 μm) were observed, and 10% addition of NaCl in foaming process had the smallest size of pores. It seems that homogeneous and heterogeneous nucleation occurred simultaneously by introducing submicron NaCl particles, even though NaCl was not an ideal nucleating agent.[32] Generally, homogeneous nucleation took place spontaneously in the bulk of PLGA matrix as a supersaturated solution was formed. Heterogeneous nucleation involved the addition of a nucleating agent, which provided an additional surface on which nucleation could occur.[31] Herein, heterogeneous nucleation was considered to be the primary mechanism because of lower activation energy for nucleation than that of homogeneous nucleation. At NaCl mass fraction of 5% [Figure 5(a)], homogeneous nucleation was still important in the process of nucleation due to having enough room for PLGA nucleation and the growth of pores. As a result, the macropores (100–300 μm) and micropores (<10 μm) could be formed at the same time by the net effect of homogeneous and heterogeneous nucleation. As the mass fractions of NaCl were above 10% [Figure 5(b)], homogeneous nucleation could be negligible, and pores with small sizes, averaged about 20 μm, were formed according to heterogeneous nucleation. With the further

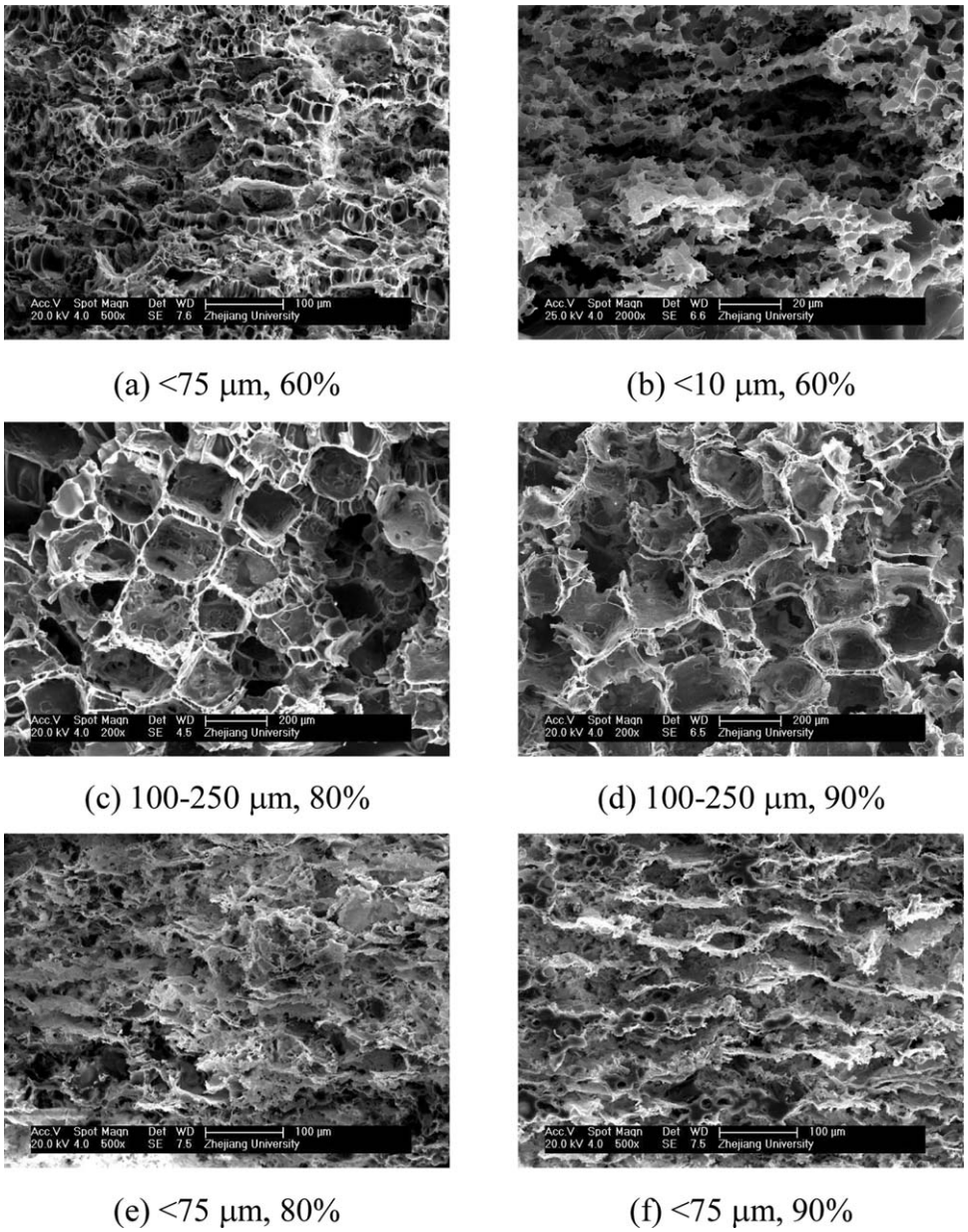

Figure 4. Effects of NaCl particle sizes and mass fractions on the morphologies of PLGA scaffolds (foaming temperature 45 °C, pressure 15 MPa).

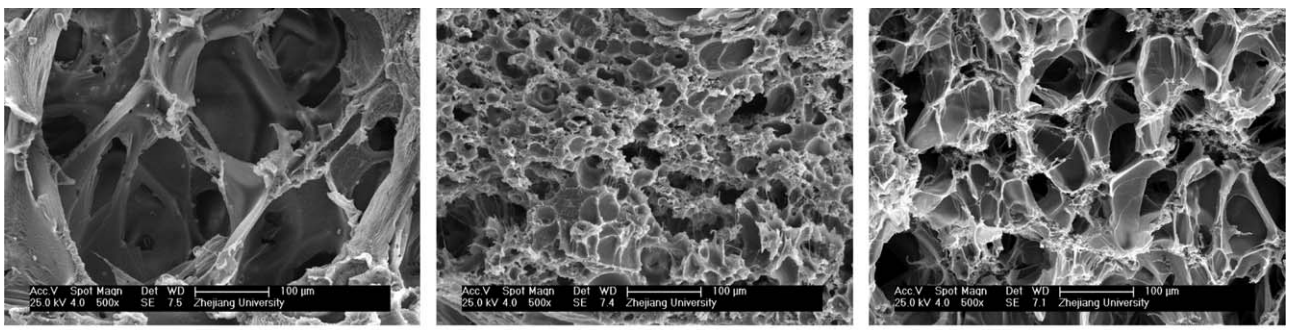

Figure 5. Nucleation and pore formation for PLGA scaffolds using submicron NaCl particles sizes as the porogen (foaming temperature 35 °C, pressure 15 MPa, NaCl particles sizes < 10 μm).

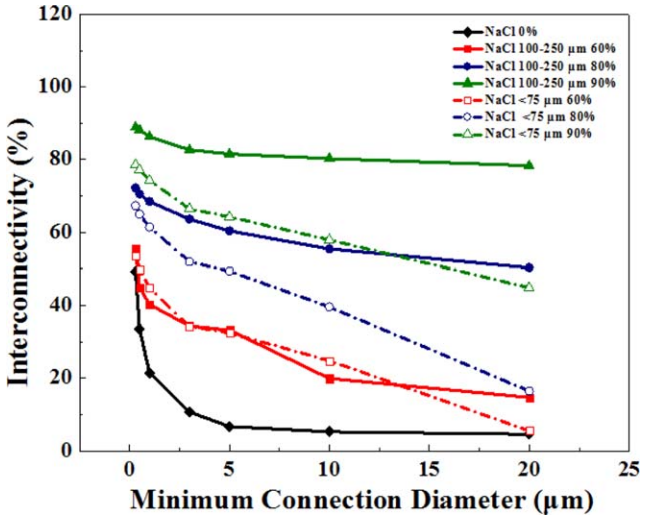

Figure 6. The interconnectivity of bimodal porous PLGA scaffolds at different minimum connection diameters using NaCl as porogen (foaming temperature 45 °C, pressure 15 MPa). [Color figure can be viewed in the online issue, which is available at wileyonlinelibrary.com.]

increase of mass fraction of NaCl to 20% [Figure 5(c)], however, the sizes of pores increased to about 100 μm due to the aggregation of NaCl particles or pore wall rupture during the pore growth.[32]

From above results, it was possible to fabricate bimodal porous scaffolds with the structure of micropores (pore size <10 μm) in the cellular walls of macropores (pore size around 100–300 μm) via heterogeneous nucleation. For this pore structure, the micropores would enhance the nutrient delivery in the porous PLGA scaffolds making macropores interconnected, and cells adhesion could be facilitated due to rough surface of macropores etched by micropores.[5] Moreover, Dorati *et al.*[8] reported that the freeze-drying process during the leaching out of NaCl particles caused the shrinkage of pores due to the molecular rearrangement of the polymer chains. Namely, even larger pores could be made when some other methods, such as vacuum drying, were chosen to postprocess scaffolds.

The Porosity and Compression Modulus of Porous Scaffolds

The porosity and compression modulus of porous scaffolds were shown in Table II. With the increase of NaCl mass fraction in Table II(a), the porosity of scaffolds raised from 68.6 ± 0.6 to 88.7 ± 0.4%, while the compression modulus decreased from 22.0 ± 1.4 to 2.2 ± 0.1 MPa. It had been well demonstrated that the mechanical properties of scaffolds were highly dependent on their porosities. Besides, the interconnectivity of pores was also an important criterion and shown in Figure 6. Generally, with the increase of minimum connection diameter, the interconnected porosity would decrease. It should be noted that when the mass fraction of NaCl (100–250 μm) was 90%, the interconnected porosity of PLGA scaffolds only decreased a little with the increase of minimum connection diameter in Figure 6. The interconnected porosity of bimodal porous scaffolds was much higher than that of PLGA scaffolds without NaCl served as porogen.[21]

The trend in Table II(b), however, was a little different. Although scaffolds fabricated had the high porosity of 79.4 ± 3.9% at a mass fraction of 5% NaCl, the compression modulus could reach up to 74.9 ± 7.9 MPa. That was due to the presence of dense surface caused by $scCO_2$ foaming.[17] As the NaCl mass fraction reached above 10%, the compression modulus decreased remarkably. This change of compression modulus might result from the effect of NaCl addition. With the increase of mass fraction of NaCl, more pores emerged on the surface of a scaffold to induce the decrease of the compression modulus. When the NaCl mass fraction increased to 20%, the compression modulus of a scaffold further decreased due to the more pores on the surface and the decrease of the thickness of pore wall.

In a whole, the bimodal porous scaffolds were fabricated with a high porosity in this study. However, the compressive modulus

Table II. Porosity and Compression Strength of Porous Scaffolds

Sizes (μm)	(a) Porosity (φ_T)%			Compression modulus (MPa)		
	NaCl 60%	NaCl 80%	NaCl 90%	NaCl 60%	NaCl 80%	NaCl 90%
100-250	69.8 ± 2.8	80.7 ± 1.8	88.7 ± 0.4	19.6 ± 0.1	5.9 ± 0.1	2.2 ± 0.1
<75	68.6 ± 0.6	74.3 ± 1.4	82.7 ± 2.8	22.0 ± 1.4	4.5 ± 0.5	2.2 ± 0.4

Sizes (μm)	(b) Porosity (φ_T)%			Compression modulus (MPa)		
	NaCl 5%	NaCl 10%	NaCl 20%	NaCl 5%	NaCl 10%	NaCl 20%
<10	79.4 ± 3.9	68.4 ± 1.4	76.3 ± 3.0	74.9 ± 7.9	0.6 ± 0.04	0.3 ± 0.1

[a] Fabricated at 45 °C, 15 MPa.
[b] Fabricated at 35 °C, 15 MPa.

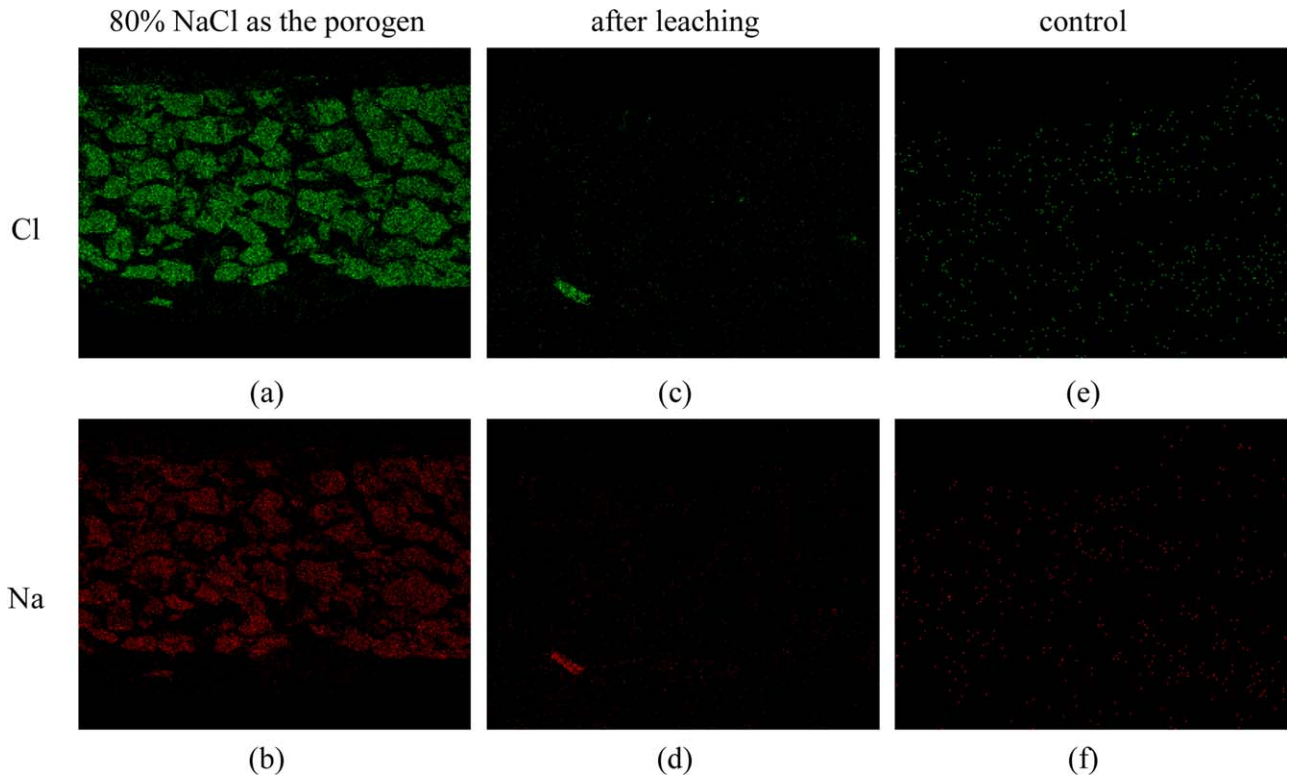

Figure 7. Elemental maps of Cl and Na in PLGA scaffolds by energy dispersive X-ray spectroscopy. [Color figure can be viewed in the online issue, which is available at wileyonlinelibrary.com.]

of fabricated porous materials could only satisfy the basic requirement of soft tissue (0.4–350 MPa) and a portion of hard tissue (10–1,500 MPa).[4] If necessary, the mechanical strength of porous scaffolds could be further improved by incorporating with hydroxyapatite or β-tricalcium phosphate to be applied in PLGA matrix.[28]

The NaCl Residual in PLGA Scaffolds

Bimodal scaffolds were fabricated by $scCO_2$ foaming/particle leaching technique in this work. It was necessary to confirm that NaCl particles were leached out completely by rinsing in deionized water, because NaCl residue would be unfavorable to cell proliferation and differentiation in scaffolds by altering osmotic pressure and electrolyte equilibrium. EDS was used to observe the NaCl residual in scaffolds, and the EDS results of scaffolds were shown in Figure 7(a,b), in which the mass fraction of NaCl (100–250 μm) was 80%. After being rinsed in deionized water for 72 h, the EDS results of scaffolds were shown in Figure 7(c,d). As a contrast, the EDS results of PLGA scaffolds without the porogen were also illustrated in Figure 7(e,f). It should be noticed that the faculae in Figure 7 were caused by background signal. From Figure 7, it could be concluded that to rinse in deionized water was an effective method to leach out NaCl particles.

In Vitro Cytotoxicity Test of PLGA Scaffolds

According to the principle of *in vitro* cytotoxicity test with GB/T 16886.5-2003, materials were deemed as toxic-free to be applied in biomedical field when RGR >50%. The results of *in vitro* cytotoxicity test of PLGA scaffolds by MTT assay were listed in Table III. When MTT assay was employed, only the viable cell populations were used to estimate the cell proliferation. As shown in Table III, PLGA scaffolds were riskless to culture cells, in which the average RGR was 89%. Therefore, scaffolds fabricated by $scCO_2$ foaming/particle leaching technique were nontoxic in tissue engineering.

CONCLUSIONS

In this work, bimodal porous scaffolds with coherent macro- and micropores structure were successfully fabricated by controlling foaming temperature, pressure, and different sizes and mass fractions of NaCl porogen. Specifically, submicron-size NaCl particles were introduced as nucleating agents to induce heterogeneous nucleation in the process of foaming. The combination of heterogeneous and homogeneous nucleation showed their typical advantages in improving the porosities of scaffolds and mechanical strength. Scaffolds prepared by $scCO_2$ foaming/particle leaching technique had no NaCl residual. Since $scCO_2$ had an ability to extract organic solvent to make scaffolds favorable to cell growth, *in vitro* cytotoxicity test of PLGA scaffolds

Table III. *In Vitro* Cytotoxicity Test of PLGA Scaffolds by MTT Assay

Samples	OD_{570}	RGR (%)
Negative control	0.363 ± 0.030	100
PLGA microspheres	0.314 ± 0.016	86
PLGA scaffolds	0.325 ± 0.014	89
Positive control	0.074 ± 0.012	20

showed these non-toxic scaffolds could be friendly applied in tissue engineering. Thus, the modified $scCO_2$ foaming/particle leaching technique was a green process and promising for fabrication of porous foams in biomedical engineering and other related fields.

ACKNOWLEDGMENTS

The authors thank gratefully for financial support by the National Natural Science Foundation of China (No. 21276225).

REFERENCES

1. Salerno, A.; Zeppetelli, S.; Di Maio, E.; Iannace, S.; Netti, P. A. *J. Supercrit. Fluid* **2012**, *67*, 114.
2. Liu, L.; Wang, Y.; Guo, S.; Wang, Z.; Wang, W. *J. Biomed. Mater. Res. B* **2012**, *100B*, 956.
3. Zhang, J. C.; Zhang, H.; Wu, L. B.; Ding, J. D. *J. Mater. Sci.* **2006**, *41*, 1725.
4. Hollister, S. J. *Nat. Mater.* **2006**, *5*, 590.
5. Cai, Q.; Yang, J. A.; Bei, J. Z.; Wang, S. G. *Biomaterials* **2002**, *23*, 4483.
6. Dong, Z.; Li, Y.; Zou, Q. *Appl. Surf. Sci.* **2009**, *255*, 6087.
7. Mondrinos, M. J.; Dembzynski, R.; Lu, L.; Byrapogu, V. K. C.; Wootton, D. M.; Lelkes, P. I.; Zhou, J. *Biomaterials* **2006**, *27*, 4399.
8. Dorati, R.; Colonna, C.; Genta, I.; Modena, T.; Conti, B. *Polym. Degrad. Stab.* **2010**, *95*, 694.
9. Kim, T. K.; Yoon, J. J.; Lee, D. S.; Park, T. G. *Biomaterials* **2006**, *27*, 152.
10. Mou, Z. L.; Zhao, L. J.; Zhang, Q. A.; Zhang, J.; Zhang, Z. Q. *J. Supercrit. Fluid* **2011**, *58*, 398.
11. Lu, L.; Zhang, Q.; Wootton, D.; Chiou, R.; Li, D.; Lu, B.; Lelkes, P.; Zhou, J. *J. Mater. Sci. Mater. M* **2012**, *23*, 2217.
12. Zhao, K.; Tang, Y. F.; Qin, Y. S.; Luo, D. F. *J. Eur. Ceram. Soc.* **2011**, *31*, 225.
13. Mou, Z. L.; Duan, L. M.; Qi, X. N.; Zhang, Z. Q. *Mater. Lett.* **2013**, *105*, 189.
14. Wu, L. B.; Jing, D. Y.; Ding, J. D. *Biomaterials* **2006**, *27*, 185.
15. Wu, L. B.; Zhang, H.; Zhang, J. C.; Ding, J. D. *Tissue Eng.* **2005**, *11*, 1105.
16. Zhang, J. C.; Wu, L. B.; Jing, D. Y.; Ding, J. D. *Polymer* **2005**, *46*, 4979.
17. Quirk, R. A.; France, R. M.; Shakesheff, K. M.; Howdle, S. M. *Curr. Opin. Solid. State* **2004**, *8*, 313.
18. Cabezas, L. I.; Gracia, I.; de Lucas, A.; Rodríguez, J. F. *Ind. Eng. Chem. Res.* **2014**, *53*, 15374.
19. Ozdemir, E.; Sendemir-Urkmez, A.; Yesil-Celiktas, O. *J. Supercrit. Fluid* **2013**, *75*, 120.
20. Yang, G.; Su, J.; Gao, J.; Hu, X.; Geng, C.; Fu, Q. *J. Supercrit. Fluid* **2013**, *73*, 1.
21. Liu, Q. Q.; Tang, C.; Du, Z.; Guan, Y. X.; Yao, S. J.; Zhu, Z. Q. *Acta Polym. Sin.* **2013**, 174.
22. Yang, Y.; Zhao, J.; Zhao, Y.; Wen, L.; Yuan, X.; Fan, Y. *J. Appl. Polym. Sci.* **2008**, *109*, 1232.
23. Zhou, Z.; Liu, X.; Liu, Q. *J. Macromol. Sci. B* **2008**, *47*, 667.
24. Ma, Z. W.; Gao, C. Y.; Gong, Y. H.; Shen, J. C. *J. Biomed. Mater. Res. B* **2003**, *67B*, 610.
25. Vaquette, C.; Frochot, C.; Rahouadj, R.; Wang, X. *J. Biomed. Mater. Res. B* **2008**, *86B*, 9.
26. Tran, R. T.; Naseri, E.; Kolasnikov, A.; Bai, X.; Yang, J. *Biotechnol. Appl. Biochem.* **2011**, *58*, 335.
27. Sadanand, J.; Kumar, A.; Pramanik, K. *J. Biomater. Tissue Eng.* **2012**, *2*, 61.
28. Mehrabanian, M.; Nasr-Esfahani, M. *Int. J. Nanomed.* **2011**, *6*, 1651.
29. Jing, X.; Mi, H. Y.; Cordie, T.; Salick, M.; Peng, X. F.; Turng, L. S. *Ind. Eng. Chem. Res.* **2014**, *53*, 17909.
30. Tsivintzelis, I.; Angelopoulou, A. G.; Panayiotou, C. *Polymer* **2007**, *48*, 5928.
31. Colton, J.; Suh, N. *Polym. Eng. Sci.* **1987**, *27*, 485.
32. Salerno, A.; Iannace, S.; Netti, P. A. *Mater. Lett.* **2012**, *82*, 137.